

Short-range correlations in binary alloys: Spin model approach to $\text{Ag}_c\text{Au}_{1-c}$ and $\text{Ag}_c\text{Pd}_{1-c}$

I. Vilja¹ and K. Kokko^{1,2}

¹*Department of Physics and Astronomy, University of Turku, FI-20014 Turku, Finland and*

²*Turku University centre for Materials and Surfaces (MatSurf), Turku, Finland*

(Dated: 27 November 2013)

Short-range correlations in Ag-Au and Ag-Pd alloys are investigated by analyzing the *ab initio* total energy of face centered cubic (fcc) based random $\text{Ag}_c\text{Au}_{1-c}$ and $\text{Ag}_c\text{Pd}_{1-c}$. Since the information on the atomic interactions is incorporated in the energetics of alloys it is possible with a suitable model, Bethe-Peierls-Weiss model is used in the present work, to invert the problem, i.e. to obtain information on the short-range correlation from the total energy of a random system. As an example we demonstrate how site correlations can be extracted from random alloy data. Bethe-Peierls-Weiss model predicts negative (positive) first neighbor correlator for substitutional fcc Ag-Au and (Ag-Pd) alloys at low temperature which can be related to the optimal structures of $\text{Ag}_{0.5}\text{Au}_{0.5}$ (and $\text{Ag}_{0.5}\text{Pd}_{0.5}$).

I. INTRODUCTION

Short-range order (SRO) in metallic alloys may induce changes in the properties of the alloys. This topic has been a subject of research in numerous investigations.¹⁻¹⁵ In the present work we study how the random alloy data can be used to extract information of the ordering tendencies of the alloys.

For test cases we adopt Ag-Au and Ag-Pd alloys. Ag-Au alloys are widely studied both experimentally and theoretically and they are considered to be alloys whose properties are well known and can be explained within the nearest-neighbor model.^{7,14} The low-temperature short-range order of Ag-Pd has attracted theoretical research for several decades. Results supporting phase separation^{16,17} as well as ordering^{1,5,11,15,18-21} have been reported. Due to the low transition temperature predicted for the disorder-order transition direct experimental observation concerning this matter is still lacking.

In the present work, we reanalyze the Ag-X (X=Au, Pd) binary alloy systems using a spin lattice model beyond the simplest mean field (Weiss) model. We employ Bethe-Peierls-Weiss (BPW) model,²² which, in contrast to Weiss model, incorporates non-vanishing correlators of neighboring atomic sites. Therefore it is suitable for extracting ordering information on the binary system in hand. To get an overview of the feasibility of the proposed method we restrict here to the nearest-neighbor interactions combined with averaged interactions beyond the nearest-neighbor level. To go beyond the nearest neighbor formalism in exact form would increase the complexity of the calculations by 2-3 orders of magnitude. This is, however, beyond the scope of the present investigation and it is left for the future study. However, we extend the BPW model by introducing a parameter controlling the beyond-the-nearest-neighbor coupling.

II. BPW MODEL

The lattice structure of binary alloys can be modeled by spin (Ising) lattices identifying spin states ± 1 of a particular site with occupation of a given atom, say A or B. For spin model calculations one has to specify the interaction energies between the sites. This can be done, for instance, by fitting the calculated lattice quantities to the corresponding observed or simulated ones.

In the following we model Ag-X by an Ising-lattice with N sites each associated with spin $\sigma_i = \pm 1$, $i = 1, \dots, N$. We identify the spin state $\sigma_i = +1$ with the occupation of the site i by a Ag atom and $\sigma_i = -1$ with the occupation of the site i by an X atom. The average concentration of the whole lattice is fixed by requiring that there is N_+ sites with $\sigma_i = +1$ and N_- sites with $\sigma_i = -1$ ($N_+ + N_- = N$). The average concentration of Ag atoms is then $c = N_+/N$ and the expectation value over all lattice sites is

$$\langle \sigma \rangle = \frac{\sum_i \sigma_i}{N} = \frac{N_+ - N_-}{N} = 2c - 1. \quad (1)$$

Considering only two-particle interactions the state sum is

$$Z = \sum_{\{\sigma_i\}_{i=1}^N} e^{-\beta E}, \quad (2)$$

where the sum is over all spin configurations with constraint $\sum_i \sigma_i = (2c-1)N$ and $\beta = (k_B T)^{-1}$, k_B is the Boltzmann constant and T temperature. The total energy (E) is written as the sum of pairwise interaction energies

$$E = \frac{1}{2} \sum_{i \neq j} E_{ij} = \sum_{i > j} E_{ij}. \quad (3)$$

An important quantity measuring the ordering of spins is the correlator

$$g_{i,j} = \langle \sigma_i \sigma_j \rangle - \langle \sigma_i \rangle \langle \sigma_j \rangle. \quad (4)$$

Here $g_{i,j} \in [-1, 1]$, $g_{i,j} < 0$ (> 0) corresponds to spins at sites i and j tending to align antiparallel (parallel), whereas the case $g_{i,j} = 0$ corresponds to completely random alignment.

In practise to calculate the state sum in Eq. (2) one has to make further approximation. In the following we use the nearest neighbor (NN) approximation, where only the closest atom sites are included in the energy sum (3). While Ising models include only two-site interactions, our task requires to include the multi-site interactions to the model. Formally this is done by allowing the Ising model parameters to depend on the concentration c , so that many-site interactions are effectively and on the average taken into account.

Thus in NN-models only the nearest neighbor sites contribute to the energy and for a fixed concentration c only effective energy for a site is given. For that purpose we define the pair interaction energy as

$$E_{ij} = \begin{cases} \epsilon(c) + \Delta\epsilon(c) \sigma_i \sigma_j + \frac{1}{2} \bar{\epsilon}(c) (\sigma_i + \sigma_j) & i, j \text{ are NN} \\ 0 & \text{otherwise} \end{cases} \quad (5)$$

Suppose now, that the site i of the Ising-lattice has ν_i nearest neighbors $j \in \mathcal{N}_i$. This number ν_i is the coordination number of the site i . Then the energy of the whole system is

$$E = \frac{1}{2} \sum_{i \neq j} E_{ij} = \frac{1}{2} \sum_{i=1}^N \sum_{j \in \mathcal{N}_i} E_{ij} = \frac{1}{2} \sum_{i=1}^N E_i, \quad (6)$$

where

$$E_i = \sum_{j \in \mathcal{N}_i} E_{ij} \quad (7)$$

is the effective energy of the site i . In this sum there is ν_i addends and reads for (5) as

$$E_i = \nu_i \left(\epsilon + \frac{1}{2} \bar{\epsilon} \sigma_i \right) + \left(\Delta\epsilon \sigma_i + \frac{1}{2} \bar{\epsilon} \right) \sum_{j \in \mathcal{N}_i} \sigma_j. \quad (8)$$

To go beyond mean field models we treat the system by BPW model.²² In BPW model each site i interacts with its ν nearest neighbors²³ $i1, \dots, i\nu$, which in part interact with their NN's other than i itself, i.e. with $\nu - 1$ sites. The interaction energy of neighbors of i are included exactly, whereas the interaction of the neighbors with their neighbors is calculated using mean field. Thus, instead of Eq. (7) the energy of a site i is

$$\begin{aligned} E_i &= \sum_{j \in \mathcal{N}_i} E_{ij} + k \sum_{j \in \mathcal{N}_i} \sum_{l \in \mathcal{N}_j, l \neq i} \langle E_{jl} \rangle_{\sigma_l} \\ &= \nu \epsilon + \frac{1}{2} \bar{\epsilon} \nu \sigma_i + \left(\Delta\epsilon \sigma_i + \frac{1}{2} \bar{\epsilon} \right) (\sigma_{i1} + \dots + \sigma_{i\nu}) \\ &\quad + k (\nu - 1) \left[\nu \epsilon + \left(\Delta\epsilon \langle \sigma \rangle + \frac{1}{2} \bar{\epsilon} \right) (\sigma_{i1} + \dots + \sigma_{i\nu}) \right. \\ &\quad \left. + \frac{1}{2} \nu \bar{\epsilon} \langle \sigma \rangle \right], \end{aligned} \quad (9)$$

where k is the control parameter regulating the importance of the next-to-nearest interactions of the basic cluster. The choice $k = 1$ corresponds to the normal BPW model. For Ag-Pd the effective pair interactions just at the first two coordination shells are needed to qualitatively understand the ordering energy,¹⁹ while in the Ag-Au system the first coordination shell is the most dominant.^{7,8,14} Moreover the parameter k can be used to obtain specific thermodynamic quantities by differentiation.

For ν NNs of site i we denote the number of $\sigma_{ij} = +1$ by n_+ and the number of $\sigma_{ij} = -1$ by n_- , so that $n_+ + n_- = \nu$ and

$$\begin{aligned}
E_i &= E(\sigma_i, n_+) \equiv \nu \epsilon + \frac{1}{2} \bar{\epsilon} \nu \sigma_i + (\Delta \epsilon \sigma_i + \frac{1}{2} \bar{\epsilon})(n_+ - n_-) \\
&\quad + k(\nu - 1) [\nu \epsilon + (\Delta \epsilon \langle \sigma \rangle + \frac{1}{2} \bar{\epsilon})(n_+ - n_-) + \frac{1}{2} \nu \bar{\epsilon} \langle \sigma \rangle] \\
&= \nu \left[\epsilon - \frac{1}{2} \bar{\epsilon} + k(\nu - 1) \left\{ \epsilon - \Delta \epsilon \langle \sigma \rangle - \frac{1}{2} \bar{\epsilon} (1 - \langle \sigma \rangle) \right\} \right] \\
&\quad + \nu \left[\frac{1}{2} \bar{\epsilon} - \Delta \epsilon \right] \sigma_i \\
&\quad + \left[\Delta \epsilon \sigma_i + \frac{1}{2} \bar{\epsilon} + k(\nu - 1) \left\{ \Delta \epsilon \langle \sigma \rangle + \frac{1}{2} \bar{\epsilon} \right\} \right] 2n_+.
\end{aligned} \tag{10}$$

When $n_+ \ll N_+$ and $\nu \ll N$ we may approximate that configuration of the ν neighbors of a fixed site i is effectively independent on all other sites. This is the main idea of Bethe-Peierls approximation.²⁴ However, BPW-approximation is widely used to model short-range correlation in various statistical systems.^{25,26} The accuracy of this approximation is however not clear, as there is no known error estimation method; PBW model has an uncontrolled error.

There would be two straightforward possibilities for next step improvement of the model beyond the BPW-approximation. By increasing the number of the exact interactions, one may extend the exact cluster in the spirit of Bethe lattice by including the interactions between NN's and their NN's, whose other interactions are included as effective mean field interactions. In the case of FCC lattice, where $\nu = 12$, the size of exact cluster is $\nu^2 - 3\nu + 1 = 109$ sites, the number of exact interactions is $\nu^2 = 144$ and effective interactions $\nu(2 \ni -11) = 156$. However, as all interactions are between NN's only, the structure of the lattice is taken in the account at the same level as in the BPW model: only the (first) coordination number defines the structure. Another possibility is to include exact interactions with the second neighbors within the exact cluster. For the second coordination number $\nu_2 (= 6$ for FCC) the exact cluster size is $\nu + \nu_2 + 1 = 19$, the number of exact interactions is $5\nu + \nu_2 = 66$ and mean field interactions is $\nu(\nu + \nu_2) + 3\nu + 7\nu_2 = 186$. This approach carries more information on the lattice structure but is more complicated to calculate due to two kind interactions it includes. Both approaches are in principle simple but technically difficult and therefore not discussed here. By going beyond the BPW-approximation there are several possibilities to improve the calculations. As far as Bethe lattice is considered, the accuracy of the approximation may be improved using cavity method of Mézard, Parisi and Virasoro²⁷, or its extensions.²⁸ Moreover, renormalization group inspired generalizations of inverse spatial dimension expansion may also upgrade the accuracy of the approximation.²⁹

Anyway, with the assumption of effective independence of neighbors of separate sites leads to BPW-partition function

$$Z = \sum_{\{\sigma_k\}_{k=1}^N} \prod_{i=1}^N e^{-\frac{1}{2} \beta E_i} = \binom{N}{N_+} Z_1(+1)^{N_+} Z_1(-1)^{N_-}. \tag{11}$$

The effective one site (neighbor) partition function for spin σ can be calculated using grand canonical ensemble of its neighbors. We write

$$Z_1(\sigma) = \sum_{n_+=0}^{\nu} \binom{\nu}{n_+} e^{\mu' n_+} e^{-\frac{1}{2} \beta E(\sigma, n_+)}. \tag{12}$$

The chemical potential of a site μ' has to be related to the overall concentration c , as N_+ is still fixed by overall concentration condition $c = N_+/N$.

Here the partition function Z is a grand canonical partition function with respect to the number of $\sigma = +1$ sites of the system but canonical one with respect to the total number of sites. That is, the partition function is related to grand potential

$$\Omega = -\frac{1}{\beta} \ln Z.$$

Thus when we later turn to use Helmholtz free energy (i.e fixed concentration) we have to make the appropriate Legendre transformation.

The thermodynamical quantities are to be calculated from the logarithm of the partition function, i.e.

$$\begin{aligned}
\ln Z &= \ln \binom{N}{N_+} \\
&- \frac{1}{2} N \beta [E_0 + c \Delta E(+1) + (1-c) \Delta E(-1)] \\
&+ N \left\{ \nu c \ln [1 + z e^{-\beta \tilde{E}_+}] \right. \\
&\left. + \nu (1-c) \ln [1 + z e^{-\beta \tilde{E}_-}] \right\}
\end{aligned} \tag{13}$$

with

$$\begin{aligned}
E_0 &= \nu \left[\epsilon - \frac{1}{2} \bar{\epsilon} \right. \\
&\left. + k(\nu - 1) \left\{ \epsilon - \Delta \epsilon \langle \sigma \rangle - \frac{1}{2} \bar{\epsilon} (1 - \langle \sigma \rangle) \right\} \right] \\
&= \nu \left[\nu_* \epsilon - \nu_* \frac{1}{2} \bar{\epsilon} + k(\nu - 1) \left\{ \frac{1}{2} \bar{\epsilon} - \Delta \epsilon \right\} \langle \sigma \rangle \right] \\
\Delta E(\sigma) &= \Delta E \sigma = \nu \left[\frac{1}{2} \bar{\epsilon} - \Delta \epsilon \right] \sigma, \\
\tilde{E}(\sigma) &= \Delta \epsilon \sigma + \frac{1}{2} \bar{\epsilon} + k(\nu - 1) \left\{ \Delta \epsilon \langle \sigma \rangle + \frac{1}{2} \bar{\epsilon} \right\} \\
&= \Delta \epsilon \sigma + \nu_* \frac{1}{2} \bar{\epsilon} + k(\nu - 1) \Delta \epsilon \langle \sigma \rangle
\end{aligned}$$

where $z = e^{\mu'}$ is the one-site fugacity

$$\begin{aligned}
z^{-1} &= \frac{\sqrt{\langle \sigma \rangle^2 + (1 - \langle \sigma \rangle^2) e^{-\beta(\tilde{E}_+ - \tilde{E}_-)} - \langle \sigma \rangle}}{1 + \langle \sigma \rangle} e^{-\beta \tilde{E}_-} \\
&= \frac{\sqrt{\langle \sigma \rangle^2 + (1 - \langle \sigma \rangle^2) e^{-2\beta \Delta \epsilon} - \langle \sigma \rangle}}{1 + \langle \sigma \rangle} e^{-\beta \tilde{E}_-},
\end{aligned} \tag{14}$$

$\tilde{E}_\pm = \tilde{E}(\pm 1)$, and $\nu_* = 1 + k(\nu - 1)$. The internal energy reads

$$\begin{aligned}
U &= -\frac{\partial \ln Z}{\partial \beta} = \frac{1}{2} N [E_0 + (2c - 1) \Delta E] \\
&+ N \left[\frac{c \nu \tilde{E}_+}{1 + z^{-1} e^{\beta \tilde{E}_+}} + \frac{(1-c) \nu \tilde{E}_-}{1 + z^{-1} e^{\beta \tilde{E}_-}} \right].
\end{aligned} \tag{15}$$

Now we turn to use fixed concentration, whence the Helmholtz free energy is given by

$$F = \Omega + \frac{\mu'}{\beta} \frac{\partial \ln Z}{\partial \mu'} = -\frac{1}{\beta} \ln Z + \frac{1}{\beta} N_+ \nu \ln z \tag{16}$$

which can be expressed as energy density. The formula for the entropy can be given after that in a standard way:

$$\begin{aligned}
TS &= U - F = U + \frac{1}{\beta} \ln Z - \frac{1}{\beta} N_+ \nu \ln z \\
&= TS_0 + \frac{N\nu}{\beta} [cI_+ + (1-c)I_- - c \ln z],
\end{aligned} \tag{17}$$

where

$$I_\pm = \frac{\beta \tilde{E}_\pm}{1 + z^{-1} e^{\beta \tilde{E}_\pm}} + \ln [1 + z e^{-\beta \tilde{E}_\pm}]. \tag{18}$$

Further, the entropy per site is

$$s = s_0 + k_B \nu [cI_+ + (1 - c)I_-] - k_B \nu c \ln z \quad (19)$$

and the Helmholtz free energy per site reads as

$$f = -\frac{1}{N\beta} \ln Z + \frac{1}{\beta} \nu c \ln z.$$

The mixing energy per atom can be constructed straightforwardly as

$$u_{mix}(c) = u(c) - cu(1) - (1 - c)u(0).$$

By differentiation of (13) with respect to energy parameters $\bar{\epsilon}$ and $\Delta\epsilon$ we find

$$g_{i,i1} = [1 - \langle\sigma\rangle^2] \left[\frac{1}{1 + z^{-1}e^{\beta\bar{E}_+}} - \frac{1}{1 + z^{-1}e^{\beta\bar{E}_-}} \right]. \quad (20)$$

Thus BPW model clearly allows correlation between a site and its neighbors. Instead of the correlator one often uses the Warren-Cowley short-range-order parameter defined as

$$\alpha_{lmn} = 1 - P_{lmn}^{AB}/c_B,$$

where P_{lmn}^{AB} is the probability of finding a B atom at site lmn (indexes are in units of half of the lattice parameter) if an A atom is at site 000 and c_B is the atomic fraction of B atoms in the A - B alloy.¹⁴ The Warren-Cowley parameter and the pair correlation function are related as

$$\alpha_{110} = \frac{g_{i,i1}}{4c_Ac_B}.$$

In the present work we express neighbor dependences using Warren-Cowley parameter. Note, that the correlator and Warren-Cowley parameter coincide at $c = 0.5$.

III. RESULTS

Next step is to determine the BPW parameters ϵ , $\bar{\epsilon}$ and $\Delta\epsilon$ by fitting the internal energy to the calculated total energy of the alloys. First we consider $\text{Ag}_c\text{Pd}_{1-c}$ alloys. As the second coordination shell is important in Ag-Pd system but there is no experimental data available to quantify its significance, we set $k = 1$ in the first place. The reference data we are using are the total energies from Ref. 30 calculated for $\text{Ag}_c\text{Pd}_{1-c}$ using the exact muffin-tin orbitals (EMTO) method^{31,32} within the coherent potential approximation (CPA),^{33,34} i.e. corresponding to the mean field approximation (Table I). The EMTO method within the full-charge density (FCD) implementation is shown to be as accurate as the full-potential methods when applied for metallic alloys.^{32,35-39} Therefore, for the substitutionally disordered random alloys the FCD-EMTO-CPA method is a perfect choice. Because the *ab initio* energies in Table I refer to the *non-correlated* Ag-Pd system at 0 K temperature we have to use in the fitting procedure the non-correlated BPW energy obtained by differentiation with respect to k or equivalently from Eq. (9) as

$$u = \frac{1}{2N} \sum_{i=1}^N \langle E_i \rangle,$$

assuming that $\langle\sigma_i\sigma_j\rangle = \langle\sigma_i\rangle\langle\sigma_j\rangle = \langle\sigma\rangle^2$ ($i \neq j$). We find the non-correlated internal energy u_{nc} to be up to normalization same as in the Weiss model,

$$u_{nc}(\langle\sigma\rangle) = \frac{1}{2} \nu \nu_* [\epsilon + \bar{\epsilon}\langle\sigma\rangle + \Delta\epsilon\langle\sigma\rangle^2]. \quad (21)$$

This can be expressed as a function of concentration as

$$u_{nc}(c) = \frac{1}{2} \nu \nu_* [\epsilon_c + \bar{\epsilon}_c c + \Delta\epsilon_c c^2], \quad (22)$$

where the parameters are related by

$$\begin{aligned}
\Delta\epsilon &= \frac{1}{4}\Delta\epsilon_c, \\
\bar{\epsilon} &= \frac{1}{2}(\Delta\epsilon_c + \bar{\epsilon}_c), \\
\epsilon &= \epsilon_c + \frac{1}{2}\bar{\epsilon}_c + \frac{1}{4}\Delta\epsilon_c.
\end{aligned}
\tag{23}$$

c	$u_{nc}(c)$ [Ry]	
	Ag _c Pd _{1-c}	Ag _c Au _{1-c}
0.00	-10084.720387	-38085.823779
0.05	-10111.731714	-36713.015417
0.10	-10138.743066	-35340.206948
0.20	-10192.765913	-32594.589743
0.30	N/A	-29848.972193
0.40	-10300.812124	-27103.354389
0.50	-10354.835440	-24357.736326
0.60	-10408.858240	-21612.118011
0.70	-10462.880386	-18866.499447
0.80	-10516.901915	-16120.880636
0.90	-10570.922942	-13375.261578
1.00	-10624.943741	-10629.642276

TABLE I: The *ab initio* internal energy at 0 K of Ag_cPd_{1-c}, as obtained in Ref. 30, and that of Ag_cAu_{1-c} calculated in this work. Instead of the exchange-correlation potential, used in Ref. 30, a more recent approximation to the exchange-correlation, the revised version of the Perdew-Burke-Ernzerhof exchange correlation approximation for solids and surfaces,^{40,41} is used in Ag-Au calculations. The difference in energies of Ag is typical when using different exchange-correlation approximations in calculations.

To fit the Eq. (22) to the numerical data shown in Table I is not an unambiguous procedure. Several justified strategies can be introduced to define the concentration dependence of the parameters ϵ_c , $\bar{\epsilon}_c$, and $\Delta\epsilon_c$. We study four different fitting schemes and compare their results with the data obtained from impurity calculations for Ag-Pd system. In three first fitting schemes we take ϵ_c and $\bar{\epsilon}_c$ to be constants whereas different boundary conditions for $\Delta\epsilon_c$ are introduced.

- i) The choice $\Delta\epsilon_c(1) = \Delta\epsilon_c(0) = 0$ leads to the correct linear form of the total energy in the limit of noninteracting atoms. This leads to tenth degree interpolation polynomial for $\Delta\epsilon_c(c)$.
- ii) Since the term $c^2\Delta\epsilon_c(c)$ vanish at $c = 0$ the above constraint can be lifted to $\Delta\epsilon_c(1) = 0$. This leads to ninth degree interpolation polynomial for $\Delta\epsilon_c(c)$.
- iii) Fitting of eight degree polynomial to the data in Table I and interpreting the two terms of lowest degree as ϵ_c and $\bar{\epsilon}_c c$, now neither $\Delta\epsilon_c(0) = 0$ nor $\Delta\epsilon_c(1) = 0$.
- iv) Redlich-Kister (RK) parameterization⁴² for Eq. (22)

$$u_{nc}(c) = \frac{1}{2}\nu\nu_*[\epsilon_{RK} + \bar{\epsilon}_{RK}c + c(1-c)\Delta\epsilon_{RK}(c)].
\tag{24}$$

Part of the linear term in (22) is included to the RK-interaction term. Note, that here ϵ_{RK} and $\bar{\epsilon}_{RK}$ are constants. Thus $\epsilon_c = \epsilon_{RK}$, $\bar{\epsilon}_c = \bar{\epsilon}_{RK} + \Delta\epsilon_{RK}$ and $\Delta\epsilon_c(c) = -\Delta\epsilon_{RK}$. The RK-parameterization is symmetric in the exchange of Pd \leftrightarrow Ag.

To decide which one of the above fitting procedures describes best the energy of Ag-Pd alloy we compare the parameters $\epsilon(c)$, $\bar{\epsilon}(c)$, and $\Delta\epsilon(c)$ at both ends ($c = 0$, $c = 1$) with the corresponding calculated data of Ag-Pd. The reference parameters are shown in Table II.

	$c = 0$	$c = 1$
ϵ_{comp} [Ry]	-143.8171426	-143.8171231
$\bar{\epsilon}_{\text{comp}}$ [Ry]	-3.7515816	-3.7516004
$\Delta\epsilon_{\text{comp}}$ [μ Ry]	0.0	60.417

TABLE II: Energy parameters ϵ , $\bar{\epsilon}$ and $\Delta\epsilon$ of $\text{Ag}_c\text{Pd}_{1-c}$ obtained from Refs. 43 and 44.

c	ϵ [Ry]	$\bar{\epsilon}$ [Ry]	$\Delta\epsilon$ [μ Ry]
0.00	-143.817139	-3.75158336	-5.555558
0.05	-143.817143	-3.75159123	-9.490742
0.10	-143.817147	-3.75159910	-13.425927
0.20	-143.817154	-3.75161484	-21.296297
0.40	-143.817159	-3.75162327	-25.513510
0.50	-143.817159	-3.75162367	-25.712963
0.60	-143.817153	-3.75161104	-19.396219
0.70	-143.817144	-3.75159374	-10.747355
0.80	-143.817135	-3.75157664	-2.199074
0.90	-143.817128	-3.75156189	5.178326
1.00	-143.817123	-3.75155107	10.587963

TABLE III: Energy parameters ϵ , $\bar{\epsilon}$, and $\Delta\epsilon$ of $\text{Ag}_c\text{Pd}_{1-c}$ as a function of concentration according to the fitting scheme (iii) with $k = 1$.

It turns out that the fitting procedure (iii) gives the best overall agreement with the *ab initio* impurity data. The BPW parameters obtained from the fit (iii) are shown in Table III. Using the BPW parameters various thermodynamic and statistical quantities can be calculated for $\text{Ag}_c\text{Pd}_{1-c}$. Figures 1 and 2 show the mixing energy and the Warren-Cowley parameter at different temperatures.

At low temperatures the mixing energy and the Warren-Cowley parameter are positive suggesting that the BPW multisite interactions drive substitutional fcc Ag-Pd to favor an atom and its neighbors to be of the same type. This suggests phase separation or segregation tendency for Ag-Pd alloys within substitutional fcc structures at low temperatures in agreement with the results of Refs. 16 and 17. However, as the recent investigations of Delczeg-Cirjak et al.⁴⁵ show the ground state structure of $\text{Ag}_{0.5}\text{Pd}_{0.5}$ is not a substitutional fcc type structure but the $L1_1$ type structure with c/a larger than its ideal value. Here c and a are the lattice parameters in hexagonal representation. In conventional cubic coordinate system c axis is along the [111] direction and the lattice parameter a is in the (111) plane. For ideal fcc structure $c/a = \sqrt{6}$, where c is the diagonal of the conventional cube and a is the nearest neighbor distance. Since the $L1_1$ structure is composed of alternating Ag and Pd (111) layers the increasing of c/a compared to the ideal value means, that the nearest neighbor distance of unlike pairs becomes larger than that of like pairs. This shifts more weight on the like-pair interaction than on the mixed-pair interaction. Therefore, the results of BPW model are consistent with the predicted tendency of $\text{Ag}_{0.5}\text{Pd}_{0.5}$ at lower temperatures to order in $L1_1$ structure with increased c/a .

At medium temperatures (50 – 100 K) the mixing energy is negative but the maximum at about $c = 0.5$ suggests a slight tendency of phase separation. At high temperatures the BPW mixing energy approaches the experimental mixing enthalpy⁴⁶ which has its minimum at about $c = 0.6$.

As a further test of the feasibility of the present method we perform the above survey also for Ag-Au alloys which differ from Ag-Pd alloys in many respects: The lattice parameters of Ag and Au are quite similar whereas the lattice parameter of Pd is considerably smaller than that of Ag. The atomic number of Au is much larger than that of Ag which leads to a steep slope in the internal energy of Ag-Au (Table I). The steep slope of the internal energy combined with the small mixing energy makes the fitting procedure more challenging for the Ag-Au systems compared to the Ag-Pd case. The mixing energy of Ag-Au is almost symmetric with the minimum at 50 at. % Ag compared to the skew shaped mixing energy with the minimum at about 60 at. % Ag in Ag-Pd alloys. The topology of the Fermi surface as a function of the concentration is also different in these two alloys. While in Ag-Au the valence d-band is completely filled within the whole concentration range, in Ag-Pd the top of the valence d-band is pushed above the Fermi energy as the Pd content is increased. Ag-Pd and Ag-Au show also different ordering behaviour at low

temperature. At $c = 0.25$ Ag-Pd is predicted to have $L1_1^+$ structure¹¹ whereas Ag-Au has the $L1_2$ structure. At $c = 0.50$ the low temperature structures of Ag-Pd and Ag-Au are $L1_1$ and $L1_0$, respectively.

As Ag-Au interactions are dominated by first coordination shell, we leave control parameter k free. The energy parameters obtained from (22) as a function of concentration (ϵ , $\bar{\epsilon}$ and $\Delta\epsilon$, Table IV) of Ag-Au are calculated using the *ab initio* internal energy of Ag-Au (Table I) and the fitting scheme (iii) with $k = 1$. More generally, energy parameters for $k \neq 1$ are to be calculated by scaling $\epsilon \rightarrow \frac{\nu}{\nu_*}\epsilon$ etc. In Table V the pair correlation function ($g_{i,i1}$) and Warren-Cowley short-range-order parameter (α_{110}) for the typical structures of Ag-Pd and Ag-Au alloys are shown.

c	ϵ [Ry]	$\bar{\epsilon}$ [Ry]	$\Delta\epsilon$ [\mu Ry]
0.00	-338.301871	190.667987	83.68056
0.05	-338.301874	190.667981	80.55556
0.10	-338.301877	190.667974	77.43056
0.20	-338.301883	190.667962	71.18055
0.30	-338.301886	190.667955	67.97839
0.40	-338.301890	190.667948	64.19270
0.50	-338.301893	190.667942	61.29166
0.60	-338.301895	190.667938	59.02777
0.70	-338.301897	190.667934	57.22789
0.80	-338.301898	190.667931	55.76714
0.90	-338.301900	190.667929	54.56532
1.00	-338.301901	190.667927	53.55208

TABLE IV: Energy parameters ϵ , $\bar{\epsilon}$, and $\Delta\epsilon$ of Ag_cAu_{1-c} as a function of concentration according to the fitting scheme (iii).

c	alloy	structure	$\langle \sigma_i \rangle$	$\langle \sigma_{i1} \rangle$	$\langle \sigma_i \sigma_{i1} \rangle$	$g_{i,i1}$	α_{110}
0.00	Au, Pd	A1	-1	1	0	0	
	Ag-Au, Ag-Pd	d.o.	-0.5	0.25	0	0	
0.25	Ag ₁ Au ₃	L1 ₂	-0.5	0	-0.25	-0.33	
	Ag ₁ Pd ₃	L1 ₁ ⁺	-0.5	0.25	0	0	
	Ag-Au, Ag-Pd	d.o.	0	0	0	0	
0.50	AgAu	L1 ₀	0	-0.33	-0.33	-0.33	
	AgPd	L1 ₁	0	0	0	0	
	Ag-Au, Ag-Pd	d.o.	0.5	0.25	0	0	
0.75	Ag ₃ Au ₁ , Ag ₃ Pd ₁	L1 ₂	0.5	0	-0.25	-0.33	
1.00	Ag	A1	1	1	0	0	

TABLE V: Correlator $g_{i,i1}$ and Warren-Cowley short-range-order parameter α_{110} for binary alloy A_cB_{1-c} ($A=Ag$, $B=Au/Pd$ $\sigma(A) = +1$, $\sigma(B) = -1$) calculated for the typical structures found in Ag-Pd and Ag-Au alloys, here d.o. refers to disordered system.

We have studied Warren-Cowley parameter at $T = 500$ K for several different values of the control parameter k and compared it with the experimental value at $c = 0.5, T = 502$ K read out from Table VI. Evidently the case $k = 1$ representing the full coupling of the neighbors to the average field overestimates the importance of the second coordination shell; the Warren-Cowley parameter ($\alpha_{110} = -0.0097$) is far too large compared to the experimental value. Likewise $k = 0$ ignoring totally the second coordination shell contribution leads astray as the Warren-Cowley parameter $\alpha_{110} = -0.1156$ is too small. The BPW model optimal value coinciding with the measured Warren-Cowley parameter is achieved when $k = 0.039$. This reflects the dominant contribution of the nearest neighbors with a small but non-ignorable effect of the next-to-nearest sites. The curves for the three cases $k = 1$, $k = 0.039$ and $k = 0$ are presented in Fig. 3. The $k = 0.039$ result compares well with the theoretical value shown in Ref. 47.

The Warren-Cowley parameters of Ag-Au calculated using the BPW results for the nearest neighbor correlator $g_{i,i1}$ with $k = 0.039$ are collected into Table VI for some values of Ag content c . Experimental results are also shown for comparison. For $c = 0.25$ and 0.50 the agreement with experiments is good but for $c = 0.75$ the BPW α_{110}

is somewhat higher than the corresponding experimental value. The BPW results can also be compared with the ordering transition temperature calculated by using the Monte Carlo method. As seen in Table V the α_{110} parameter is -0.33 for the ordered $L1_0$ and $L1_2$ structures. The BPW model predicts α_{110} of this magnitude at slightly above 100 K for $c = 0.50$ in agreement with the Monte Carlo transition temperature. For $c = 0.25$ and 0.75 the BPW model predicts transition temperatures to be about 50 K which is considerably lower than the Monte Carlo results. Moreover, Fig. 4 shows the calculated mixing energy of Ag-Au at various temperatures showing good agreement with other theoretical and experimental results.^{3,46-49}

T [K]	c		
	0.25	0.50	0.75
20	-0.3392	-0.9661	-0.3388
50	-0.3207	-0.6708	-0.3053
100	-0.2432	-0.3851	-0.2145
300	-0.1035	-0.1345	-0.0862
500	-0.0646	-0.0810	-0.0533
	(488 K)	(502 K)	(513 K)
exp.	(25.0 at.%)	(47.7 at.%)	(74.7 at.%)
	-0.0677	-0.0810	-0.0720
$L1_2, L1_0 \leftrightarrow$ d.o.	155 K	115 K	115 K

TABLE VI: The nearest neighbor Warren-Cowley short-range-order parameters (α_{110}) of $\text{Ag}_c\text{Au}_{1-c}$ calculated using the BPW nearest neighbor correlator $g_{i,i1}$ with $k = 0.039$. Bottom part of the Table shows experimental results of α_{110} based on diffuse x-ray scattering data and Monte Carlo order-disorder transition temperatures based on effective potentials obtained by using experimental short-range order parameters.¹⁴

IV. SUMMARY

We have used the Bethe-Peierls-Weiss model to investigate the effect of multisite interactions on the ordering in $\text{Ag}_c\text{Pd}_{1-c}$ and $\text{Ag}_c\text{Au}_{1-c}$ alloys. The mean field *ab initio* data has been used to determine the parameters of the BPW model. The BPW mixing energy, neighbor correlator and nearest-neighbor Warren-Cowley short-range-order parameter for substitutional fcc alloys of Ag-Pd and Ag-Au have been calculated. The correlator of Ag-Pd is positive at low temperatures supporting the stability of the $L1_1$ structure of $\text{Ag}_{0.5}\text{Pd}_{0.5}$ with elongation along the hexagonal [111] axis. For Ag-Au the BPW model predicts the short-range order and order-disorder transition temperature for $c = 0.50$ alloy quite well compared to experiments and other theoretical results. For $c = 0.25$ and 0.75 alloys the BPW model predicts the short-range-order parameter reasonably well but the BPW order-disorder transition temperature for these alloys is too low. Some straightforward extensions of the BPW-model to a larger exact cluster may remedy these inaccuracies. In spite of this, the presented BPW formalism is shown to be a promising technique to extract and analyze the short-range order of random substitutional metallic alloys using as an input the mixing energies at the mean field approximation level.

¹ A. Gonis, W. H. Butler, and G. M. Stocks, Phys. Rev. Lett. **50**, 1482 (1983).

² A. Raoufi, S. Arajs, and K. V. Rao, phys. stat. sol. (a) **97**, 571 (1986).

³ T. Mohri, K. Terakura, T. Oguchi, and K. Watanabe, Acta Metall. **36**, 547 (1988).

⁴ Z. W. Lu, S.-H. Wei, and A. Zunger, Phys. Rev. B **44**, 10470 (1991).

⁵ Z. W. Lu, S.-H. Wei, A. Zunger, S. Frota-Pessoa, and L. G. Ferreira, Phys. Rev. B **44**, 512 (1991).

⁶ T. Mohri, K. Terakura, S. Takizawa, and J. M. Sanchez, Acta Metall. Mater. **39**, 493 (1991).

⁷ Z. W. Lu, B. M. Klein, and A. Zunger, Modelling Simul. Mater. Sci. Eng. **3**, 753 (1995).

⁸ V. Ozoliņš, C. Wolverton, and A. Zunger, Phys. Rev. B, **57**, 6427 (1998).

⁹ C. Wolverton, V. Ozoliņš, and A. Zunger, J. Phys.: Condens. Matter **12**, 2749 (2000).

¹⁰ I. R. Yukhnovskii, Z. A. Gurskii, and Ya. G. Chushak, phys. stat. sol. (b) **163**, 107 (1991).

¹¹ S. Müller and A. Zunger, Phys. Rev. Lett. **87**, 165502 (2001).

¹² L. Wang, X.-F. Bian, and J.-X. Zhang, Materials Science and Engineering, materials Science and Engineering **A298**, 262 (2001).

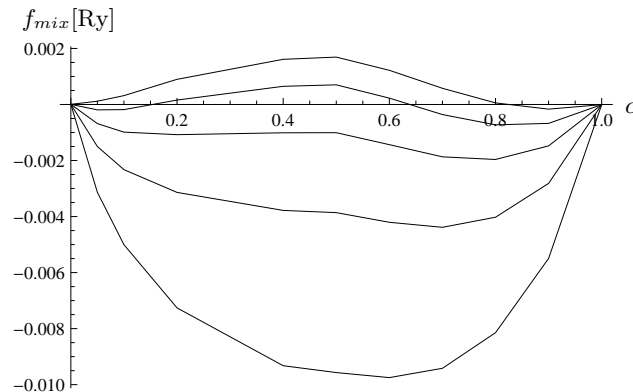


FIG. 1: (Color online) Helmholtz free mixing energy per site f_{mix} of $\text{Ag}_c\text{Pd}_{1-c}$ at $T = 1\text{K}, 20\text{K}, 50\text{K}, 100\text{K}, 200\text{K}$ (from up to down) .

- ¹³ P. R. Tulip, J. B. Staunton, S. Lowitzer, D. Ködderitzsch, and H. Ebert, Phys. Rev. B **77**, 165116 (2008).
- ¹⁴ B. Schönfeld, J. Traube, and G. Kosterz, Phys. Rev. B **45**, 613 (1992).
- ¹⁵ M. Hoffmann, A. Marmodoro, E. Nurmi, K. Kokko, L. Vitos, A. Ernst, and W. Hergert, Phys. Rev. B **86**, 094106 (2012).
- ¹⁶ R. A. Johnson, Phys. Rev. B **41**, 9717 (1990).
- ¹⁷ N. Takano, A. Yoshikawa, and F. Terasaki, Solid State Commun. **107**, 213 (1998).
- ¹⁸ S. Curtarolo, D. Morgan, and G. Ceder, Comput Coupling Phase Diagrams Thermochem. **29**, 163 (2005).
- ¹⁹ A. V. Ruban, S. I. Simak, P. A. Korzhavyi, and B. Johansson, Phys. Rev. B **75**, 054113 (2007).
- ²⁰ S. Takizawa, K. Terakura, and T. Mohri, Phys. Rev. B **39** 5792 (1989).
- ²¹ I. A. Abrikosov and H. L. Skriver, Phys. Rev. B **47**, 16532 (1993).
- ²² P. R. Weiss, Phys. Rev. **74**, 1493 (1948).
- ²³ We suppose here again, that each site has same coordination number.
- ²⁴ H. S. Robertson, *Statistical Thermophysics* (Prentice-Hall, New Jersey, 1993).
- ²⁵ T. Vojta and W. John, J. Phys.: Condens. Matter **5**, 57 (1993).
- ²⁶ T. Vojta, W. John and M. Sreiber, J. Phys.: Condens. Matter **5**, 4989 (1993).
- ²⁷ M. Mézard, G. Parisi and M. A. Virasoro, Europhys. Lett. **1**, 77 (1986); M. Mézard and G. Parisi, J. Stat. Phys. **111**, 1 (2003).
- ²⁸ See, e.g.: J.S. Yedidia, W.T. Freeman and Y. Weiss, Advances in Neural Information Processing Systems bf 13, 689 (2001).
- ²⁹ See, e.g.: A. Georges and J. Yedidia, J. Phys. A: Math. Gen. **24**, 2173 (1991).
- ³⁰ M. Ropo, K. Kokko, L. Vitos and J. Kollár, Phys. Rev. B **71**, 45411 (2005).
- ³¹ L. Vitos, *Computational Quantum Mechanics for Materials Engineers: The EMTO Method and Applications*, Engineering Materials and Processes Series (Springer-Verlag, London, 2007).
- ³² L. Vitos, I. A. Abrikosov, and B. Johansson, Phys. Rev. Lett. **87**, 156401 (2001).
- ³³ P. Soven, Phys. Rev. **156**, 809 (1967).
- ³⁴ B. L. Györfy, Phys. Rev. B **5**, 2382 (1972).
- ³⁵ L. Vitos, Phys. Rev. B **64**, 014107 (2001).
- ³⁶ B. Magyari-Köpe, G. Grimvall, and L. Vitos, Phys. Rev. B **66**, 064210 (2002); **66**, 179902(E) (2002).
- ³⁷ A. Taga, L. Vitos, B. Johansson, and G. Grimvall, Phys. Rev. B **71**, 014201 (2005).
- ³⁸ A. E. Kissavos, S. I. Simak, P. Olsson, L. Vitos, and A. I. Abrikosov, Computational Materials Science **35**, 1 (2006).
- ³⁹ E. K. Delczeg-Czirjak, L. Delczeg, M. Ropo, K. Kokko, M. P. J. Punkkinen, B. Johansson, and L. Vitos, Phys. Rev. B **79** 085107 (2009).
- ⁴⁰ J. P. Perdew, A. Ruzsinszky, G. I. Csonka, O. A. Vydrov, G. E. Scuseria, L. A. Constantin, X. Zhou, and K. Burke, Phys. Rev. Lett. **100**, 136406 (2008).
- ⁴¹ M. Ropo, K. Kokko, and L. Vitos, Phys. Rev. B **77**, 195445 (2008).
- ⁴² O. Redlich and A. T. Kister, Ind. Eng. Chem. **40**, 345 (1948).

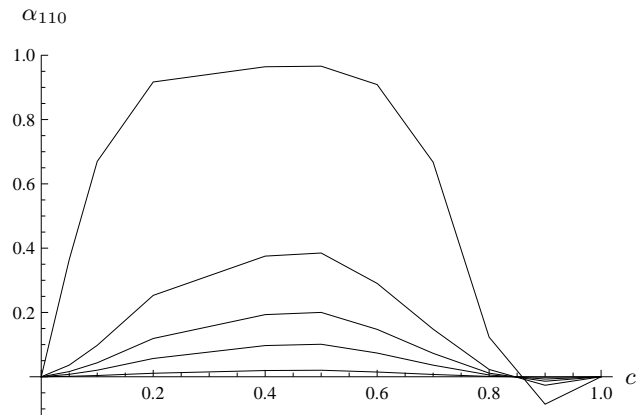


FIG. 2: (Color online) Warren-Cowley SRO parameter of $\text{Ag}_c\text{Pd}_{1-c}$ at various temperatures $T = 1\text{K}, 5\text{K}, 10\text{K}, 20\text{K}, 100\text{K}$ (from up to down).

⁴³ T. Hoshino, W. Schweika, R. Zeller, and P. H. Dederichs, *Phys. Rev. B* **47**, 5106 (1993).

⁴⁴ www.imprs-am.mpg.de/summerschool2003/skriver.pdf

⁴⁵ E. K. Delczeg-Czirjak, E. Nurmi, K. Kokko, and L. Vitos, *Phys. Rev. B* **84** 094205 (2011).

⁴⁶ R. Hultgren, P. D. Desai, D. T. Hawkins, M. Gleiser, and K. K. Kelley, *Selected Values of the Thermodynamic Properties of Binary Alloys* (American Society for Metals, Metals Park, Ohio, 1973).

⁴⁷ O. E. Awe, O. Akinlade, and L. A. Hussain, *Journal of Alloys and Compounds* **387**, 256 (2005).

⁴⁸ I. A. Abrikosov, A. V. Ruban, B. Johansson, and H. L. Skriver, *Comput. Mater. Sci.* **10**, 302 (1998).

⁴⁹ Z. W. Lu, B. M. Klein, and A. Zunger, *Modelling. Simul. Mater. Sci. Eng.* **3**, 753 (1995).

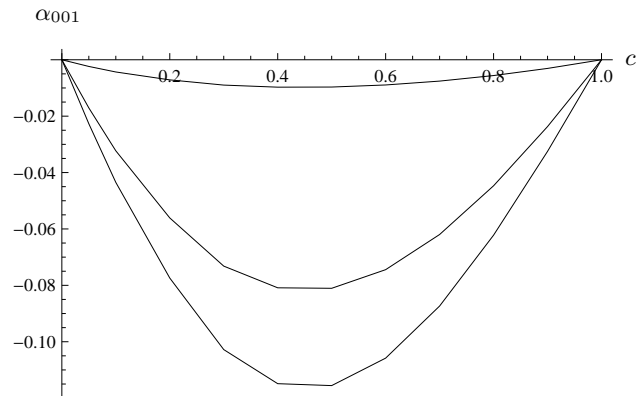


FIG. 3: (Color online) Warren-Cowley parameters of $\text{Ag}_c\text{Au}_{1-c}$ for three values of control parameter: $k = 1$, $k = 0.039$, $k = 0$ (from up to down) at 500 K.

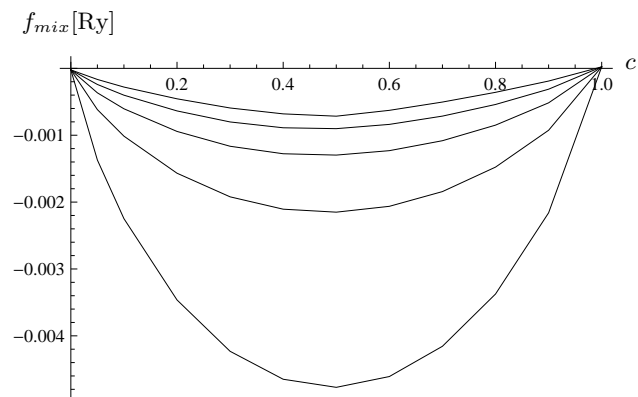


FIG. 4: (Color online) Helmholtz free mixing energy per site f_{mix} of $\text{Ag}_c\text{Au}_{1-c}$ at $T = 20\text{K}$, 50K , 100K , 200K , 500K for $k = 0.039$ (from up to down).